

# A VERY LARGE-EDDY SIMULATION (VLES) MODEL FOR INVESTIGATION OF THE THERMALLY-STRATIFIED ATMOSPHERIC BOUNDARY LAYERS: REDUCTIONIST AND PRACTICAL

Amir A. Aliabadi

Environmental Engineering, University of Guelph  
Guelph, Canada  
Corresponding Author: aliabadi@uoguelph.ca

Gonçalo Pedro  
RWDI  
Guelph, Canada

**Abstract**—A Very Large-Eddy Simulation (VLES) model was developed to simulate thermally-stratified atmospheric boundary layers. The model performance was validated against experimental wind tunnel observations. The effects of grid resolution and model input parameters were analyzed in the suitability of the model to predict the experimental observations. The model exhibited a short adaptation distance smaller than five boundary-layer heights. It produced most of the mean and turbulence statistics profiles reasonably well in agreement with the experiments. The VLES model shall be further tested at full scale to simulate thermally-stable atmospheric boundary layers. The model should also be tested on complex topography with differential surface temperature to ensure adequate performance in realistic applications.

**Keywords**-Atmospheric boundary layer; Computational Fluid Dynamics (CFD); Thermally-stratified flow; Very Large-Eddy Simulation (VLES);

## I. INTRODUCTION

In the recent decades, Large-Eddy Simulation (LES) models have gained popularity among practical CFD models with a high degree of fidelity [4]. It is true that LES models do not resolve turbulent fluctuations of a flow at all scales of the energy cascade, but they resolve the energy-containing and a significant portion of the inertial subrange scales [3, 4, 6]. Such scales of fluctuations govern important aspects of turbulent flows such as pollutant dispersion and excitation of structures immersed in flows.

Despite such popularity, one of the main difficulties in implementing realistic LES models is the lack of the availability of simplistic yet adequate perturbation fields to be inserted at the model flow inlet. LES requires such perturbations because it is the nature of this type of modelling to simulate the evolution of perturbations in a numerical domain that eventually describe the turbulent fluctuations in the flow. From a theoretical stand point, the perfectly ideal inlet

fluctuations must meet several criteria: 1) they must be stochastically varying, on scales down to the spatial and temporal filter scales; 2) they must be compatible with the Navier-Stokes equations; 3) they must be composed of coherent eddies across a range of spatial scales down to the filter length; 4) they must allow easy specification of turbulent properties; and 5) they must be easy to implement [16].

In practice, however, no simple model exists that meets all such criteria for flow inlet perturbations. Models either employ simplistic approaches while missing important physical aspects of the flow [10, 17, 15, 7, 11, 18], or they employ fully realistic methods at the expense of complexity of implementation [1, 2, 8, 14].

A reductionist yet practical model was implemented by Aliabadi et al. [6] for the investigation of neutral atmospheric boundary layers. This model was known as a Very Large-Eddy Simulation (VLES) model and employed a synthetic method for inlet perturbations. The development aimed at minimizing the number of input parameters for the model while attempting to simulate mean flow, turbulence statistics, spectra, and anisotropy realistically. The input parameters were a single timescale and a single lengthscale specifying the turbulent inlet fluctuations, a parameter controlling the Sub-Grid Scale (SGS) transport, and an aerodynamic surface roughness lengthscale. The model was tested against experimental wind tunnel data and other LES models. It produced experimental profiles of mean velocity and turbulence velocity statistics reasonably well. It simulated spectra and anisotropy realistically. This model showed potential for use in industrial applications where it is impractical to perform high resolution simulations or implement complex synthetic inlet boundary conditions to match all flow properties beyond what is necessary for a practical application.

The objective of this study is to extend the VLES model capabilities in simulating thermally-stratified atmospheric boundary layers. The model performance is validated against experimental wind tunnel observations of Ohya [12]. The effect of grid resolution is analyzed. The model performance as a

function of inlet parameters is studied in a sensitivity investigation. Various thermal stability strengths are analyzed. In addition, the model performance is investigated with the use of momentum and thermal wall functions. The VLES model is implemented in OpenFOAM 4.0.

## II. METHODOLOGY

### A. Model Geometry

The model geometry is shown in Fig. 1. The tunnel height, width, and length are  $Z=1.5\text{m}$ ,  $Y=1.5\text{m}$ , and  $X=5\text{m}$ , respectively. Airflow is in the  $x$  direction. Four vertical solution probes are considered for monitoring the simulation results. All results reported in this paper are obtained from the solutions monitored on probe 4. This choice ensures the flow is fully developed for statistical sampling.

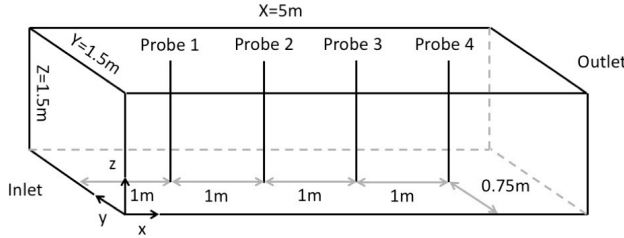


Figure 1. Model geometry.

### B. The Synthetic Vortex Method

To generate turbulence at the inlet, a vortex method is used. This method was originally developed by Sergent [15] but has been continually improved until recently [18]. In this method, velocity fluctuations are inserted at the inlet in the form of synthetic two-dimensional eddies derived from mean statistical information about the flow as a function of space (height above ground) and time. This method does neither require a precursor method to generate fluctuations beforehand using another simulation, nor require periodic streamwise boundary conditions to recycle fluctuations from inside the domain. Therefore, it offers great simplicity. The velocity fluctuation field is given as

$$u(x) = \frac{1}{2\pi} \sum_{i=1}^N \Gamma_i \frac{(x_i - x) \times s}{|x_i - x|^2} \left( 1 - e^{-\frac{|x_i - x|^2}{2(\sigma_i(x_i))^2}} \right) e^{-\frac{|x_i - x|^2}{2(\sigma_i(x_i))^2}}, \quad (1)$$

where  $u(x)$  is velocity perturbation vector at the model inlet that is later superimposed on the mean inlet velocity,  $x$  is position vector on the inlet boundary,  $N$  is the number of vortices to be inserted at the inlet (in this study 200),  $i$  is the index for the current vortex,  $\Gamma_i$  is the circulation for the current vortex,  $x_i$  is the position vector for the centre of the current vortex,  $s$  is unit vector along the streamwise direction, and  $\sigma_i(x_i)$  is characteristic length for the radius of current vortex. We assume that the wall-normal direction is  $+z$  and that flow is in the  $+x$  direction. A power-law profile is used for the mean inlet velocity

$$\bar{U}(z) = U_{ref} \left( \frac{z}{z_{ref}} \right)^\alpha, \quad (2)$$

where  $z_{ref}$  is a reference height (0.1m),  $U_{ref}$  is reference velocity, and  $\alpha$  is an exponent parameterized as a function of aerodynamic surface roughness length of the surface  $z_0$  given as

$$\alpha = \frac{1}{\ln\left(\frac{z_{ref}}{z_0}\right)}. \quad (3)$$

Next a turbulence intensity profile must be assumed. This is obtained from

$$I_u(z) = \frac{1}{\ln\left(\frac{z}{z_0}\right)}, \quad (4)$$

where  $I_u(z)$  is limited by a maximum value given the fact that for atmospheric flows there is a limit to  $I_u(z)$  of typically in the order of one. This allows parameterization of Turbulence Kinetic Energy (TKE) ( $k$ ) such that

$$k(z) = 1.5(U(z)I_u(z))^2. \quad (5)$$

Calculation of the characteristic size for energy-containing eddies begins with the calculation of inlet boundary lengthscale

$$L = \frac{2L_z L_y}{L_z + L_y} \quad (6)$$

where inlet dimensions are used. It is reasonable to assume that the size of energy-containing eddies  $\sigma_{max}$  scales with  $L$ , using a constant  $\alpha_\sigma$ , to be adjusted later, according to

$$\sigma_{max} = \alpha_\sigma L \quad (7)$$

Meanwhile, the size of energy-containing vortices or eddies is a function of height and must decrease with height. The energy-containing vortex size is parameterized using the mixing length approach

$$\frac{1}{\sigma(z)} = \frac{1}{\sigma_{max}} + \frac{1}{\kappa(z + z_0)}, \quad (8)$$

where,  $\kappa=0.41$  is the von Kármán constant. A characteristic time for the largest energy-containing eddies can be approximated using scaling. The characteristic velocity  $U_0$  for the largest energy-containing eddies can be defined using the power law and the reference height so that  $U_0 = \alpha z_{ref}^\alpha$ . The lengthscale for such eddies can be defined as  $\ell_0 = \sigma_{max}$ . Calculation of these two scales enable the calculation of the largest energy-containing eddies Reynolds number  $Re_{\ell_0} = U_0 \ell_0 / \nu$ . We can subsequently calculate the Kolmogorov length scale  $\eta = \ell_0 Re_{\ell_0}^{-3/4}$ , the Kolmogorov velocity scale  $u_\eta = U_0 Re_{\ell_0}^{-1/4}$ , and the dissipation rate  $\epsilon = \nu(u_\eta/\eta)^2$ . Finally, we can calculate the characteristic lifetime for the largest energy-containing eddies

$$\tau_0(\ell_0) = \left( \frac{\ell_0^2}{\epsilon} \right)^{1/3}. \quad (9)$$

This timescale is not representative for all energy-containing eddies, but only the largest ones. For ease of implementation,

however, it is possible to define a representative timescale for all energy-containing eddies assuming a constant  $a_\tau$ , to be adjusted later, with

$$\tau = a_\tau \tau_0 (\ell_0). \quad (10)$$

This timescale can be used to sample a new set of vortices at the inlet after every fixed number of timesteps, so that as soon as this timescale is elapsed new vortices will be sampled.

The circulation can be formulated for each vortex with the knowledge of computational face area  $S$ , in which the vortex center is located and the TKE ( $k$ ) given for a height. The circulation sign is randomized as either positive or negative such that

$$\Gamma = \pm 4 \left( \frac{\pi S k}{3N(2 \ln 3 - 3 \ln 2)} \right)^{1/2}. \quad (11)$$

The inlet temperature profile is formulated using a power law with the same exponent found earlier such that

$$\theta(z) = (\theta_\infty - \theta_s) \left( \frac{z}{z_{max}} \right)^\alpha + \theta_s, \quad (12)$$

where  $\theta_\infty$  is the far field temperature on top of the boundary layer,  $\theta_s$  is surface temperature, and  $z_{max}$  is the height for the top of the domain, i.e. above which  $\theta_\infty$  is defined.

These formulations fully close the system of equations necessary for the synthetic eddy method.

### C. The Sub-Grid Scale (SGS) Model

The Sub-Grid Scale (SGS) model is fully described by Aliabadi et al. [3]. This is based on a one-equation TKE ( $k$ ) model, for which the sub-grid lengthscale is formulated as

$$l = C_\Delta (\Delta x \Delta y \Delta z)^{1/3}, \quad (13)$$

where  $C_\Delta$  is a parameter to control  $l$  and therefore the SGS model.

### D. Wall Functions

The VLES model requires two wall functions: one for momentum transport and the other for heat transport near the walls. The wall function for momentum transport is given by Raupach et al. [13]

$$U^+ = \frac{U}{u_\tau} = \frac{1}{\kappa} \ln \left( \frac{z+z_0}{z_0} \right), \quad (14)$$

where  $u_\tau$  is friction velocity and  $z_0$  is the characteristic aerodynamic roughness length of the surface. The wall function for temperature is given by Jayatilleke [9]

$$T^+ = \frac{(T_w - T) \rho C_p u_\tau}{q_w} = Pr_t (u^+ + Pr_f), \quad (15)$$

where  $Pr_t=0.85$  is the turbulent Prandtl number. Here  $Pr_f$  is further parameterized as a function of  $Pr_t$  and the laminar Prandtl number  $Pr=0.72$

$$Pr_f = 9.24 \left[ \left( \frac{Pr}{Pr_t} \right)^{3/4} - 1 \right] \left[ 1 + 0.28 e^{\left( -0.007 \frac{Pr_t}{Pr} \right)} \right]. \quad (16)$$

### E. Numerical Schemes

The implementation of numerical grid, boundary conditions, finite volume schemes, finite volume solution control, and solution averaging are fully discussed in Aliabadi et al. [3] and Aliabadi et al. [6] and will not be provided here for brevity.

### F. Numerical Grids

Four grid levels are chosen for the simulations that vary from very fine (level I) to very coarse (Level IV). These grids are listed in Table I with appropriate descriptions and specifications.

TABLE I. NUMERICAL GRID LEVELS

Grid Level	Grid Level Information		
	Description	$N_x \cdot N_y \cdot N_z$	$N_{Total}$
I	Very fine	100-100-100	1,000,000
II	Fine	100-75-75	562,500
III	Coarse	100-50-50	250,000
IV	Very Coarse	100-25-25	62,500

### G. Validation Dataset

The validation dataset is obtained from wind tunnel experiments of Ohya [12]. For this wind tunnel a chain roughness was used with lengthscale  $h=0.0055m$  or equivalently an aerodynamic roughness length of  $z_0=0.00055m$  ( $z_0 \sim 0.1h$ ). Table II shows the details of wind tunnel experimental cases. As can be seen, the experiments are mainly run to vary the thermal stability condition, given by the bulk Richardson number  $Ri_\delta$ . In addition, the Reynolds number based on boundary layer height  $Re_\delta$  and vertical temperature difference between far field and surface  $\Delta\theta = \theta_\infty - \theta_s$  are reported. These cases correspond to very weakly stable (Case 1) to very strongly stable (Case 4) conditions.

TABLE II. WIND TUNNEL EXPERIMENTAL CASES OF OHYA (2001)

Experimental Variables	Stability Case			
	Case 1	Case 2	Case 3	Case 4
$U_\infty$ [m s <sup>-1</sup> ]	1.83	1.29	1.01	0.91
$Re_\delta$	50,600	35,300	28,000	23,700
$Ri_\delta$	0.12	0.24	0.40	0.74
$\Delta\theta = \theta_\infty - \theta_s$ [K]	27.4	27.4	28.7	43.3

## III. RESULTS

### A. Sensitivity to Grid Levels

First the VLES model has been run with a default set of synthetic eddy parameters on different grid resolutions. Fig. 2 shows the results of the analysis. It appears that most solution variables reasonably agree with the experimental wind tunnel observations for a grid level as coarse as grid level III. The choice of such a grid warrants a good agreement with experiments. However, results obtained on grid level IV

deviate from the experimental observations, suggesting that such a coarse level of a grid is not desirable. These simulations were wall resolving so that no wall function had to be used at the wall boundary. Here  $\delta$  represents the boundary-layer height, which is used to normalize vertical distance from the wall.

### B. Different Thermal Stability Cases

Next the VLES model was run with a default set of synthetic eddy parameters for different thermal stability cases according to Table II. Fig. 3 shows the results of the analysis. All stability cases were run on grid level III, which was shown to be resolved enough for this VLES model. The agreement is reasonably good. Although there are deviations from the wind tunnel observations, the VLES model predicts the same trends as the experiments for the turbulence statistics by indicating a suppression of the magnitude of such statistics with increasing thermal stability.

### C. Sensitivity to $a_\sigma$

Next the VLES model has been run in a sensitivity investigation for the choice of the  $a_\sigma$  synthetic eddy parameter. This parameter controls the size of eddies fed at the inlet. Fig. 4 shows the results of the analysis. All cases were run on grid level III. The results show that mean quantities are not affected

by varying  $a_\sigma$ ; however, using larger values of  $a_\sigma$  results in larger magnitudes of turbulence statistics. This can be explained by the fact that larger eddy structures are more energetic and overall add to the turbulence levels in the simulation domain. The choice of  $a_\sigma=3$  results in the best agreement in turbulence statistics with the wind tunnel experiments. Note that this choice is valid for wall-resolving simulations.

### D. Sensitivity to $a_\tau$

Next the VLES model has been run in a sensitivity investigation for the choice of the  $a_\tau$  synthetic eddy parameter. This parameter controls how frequently new eddies are sampled at the inlet. In other words, this parameter controls the lifetime of the largest energy-containing eddies at the inlet. Fig. 5 shows the results of the analysis. All cases were run on grid level III. The results show that mean quantities are not affected significantly by varying  $a_\tau$ ; however, using larger values of  $a_\tau$  results in larger magnitudes of turbulence statistics. The choice of  $a_\tau=0.01$  results in the best agreement in turbulence quantities. Note that this choice is valid for wall-resolving simulations.

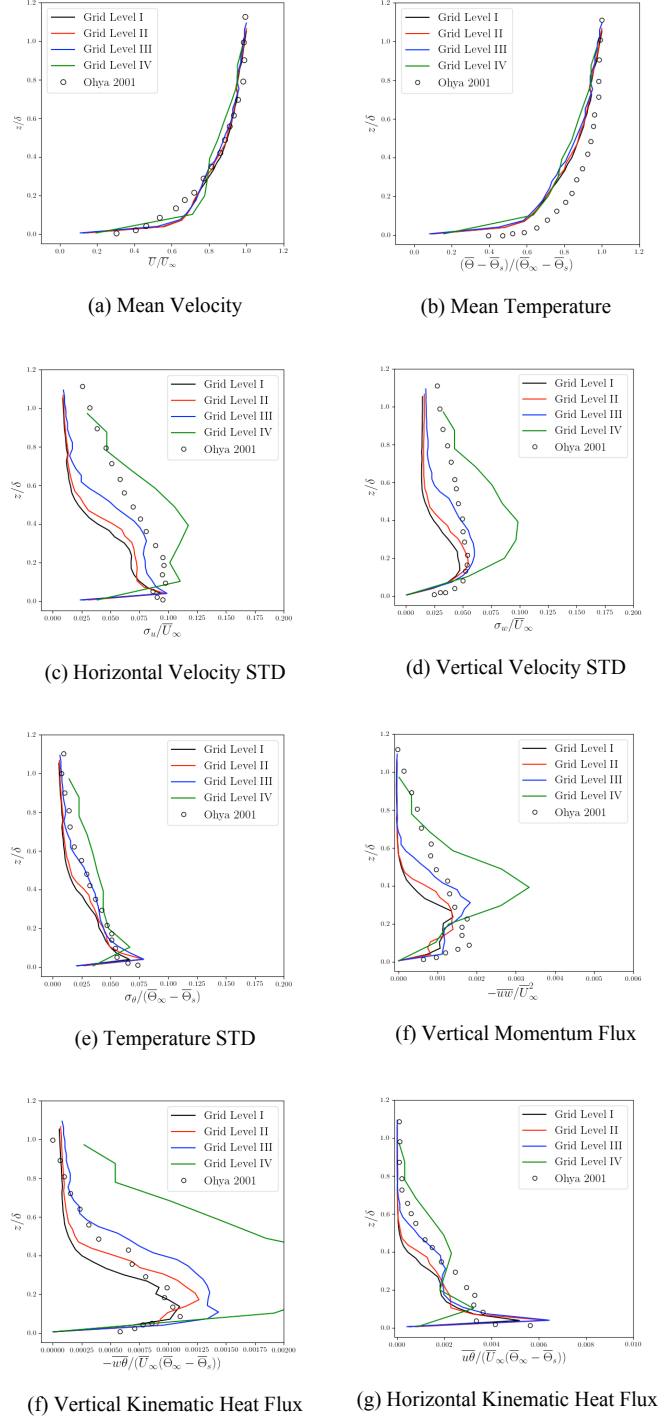


Figure 2. Sensitivity of the VLES model to grid level: very fine (Level I), fine (Level II), coarse (Level III), and very coarse (Level IV).

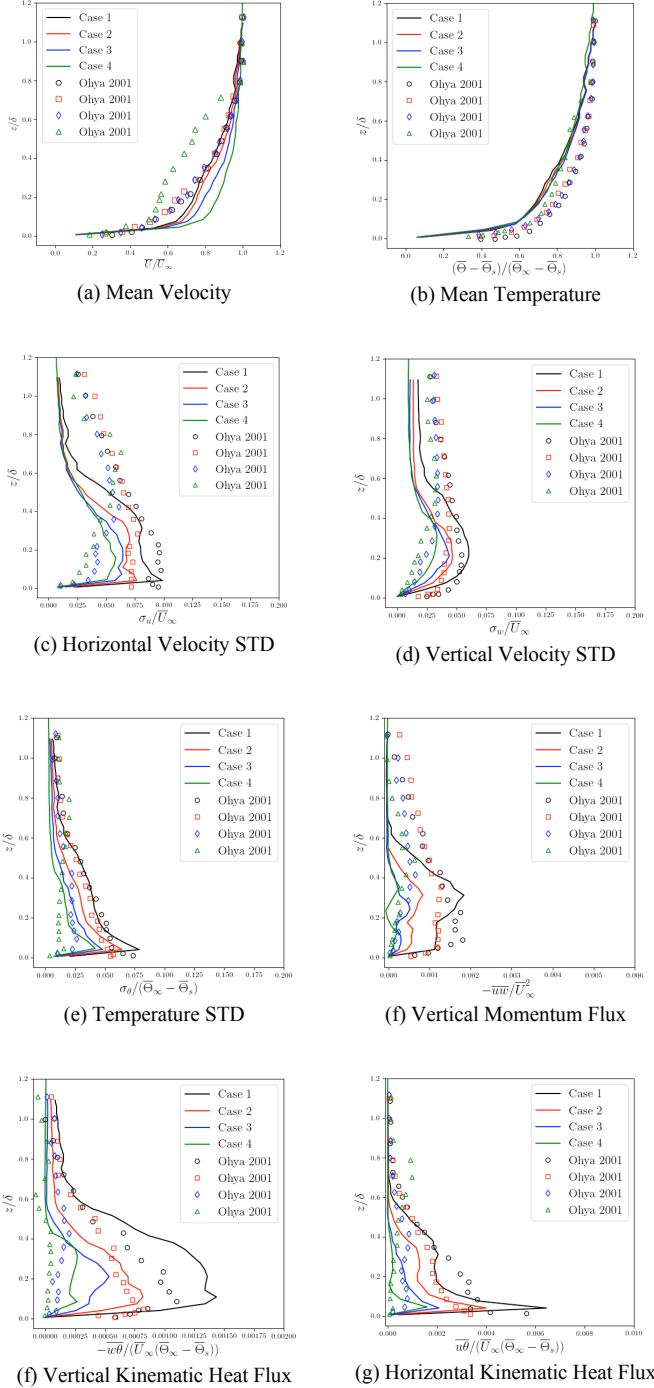


Figure 3. Response of the VLES model to different thermal stability conditions: very weakly stable (Case 1), stable (Case 2), strongly stable (Case 3), very strongly stable (Case 4).

### E. Sensitivity to $C_{\Delta}$

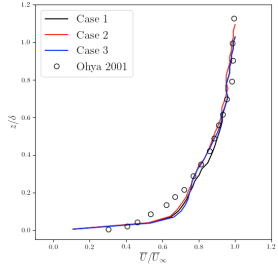
Next the VLES model has been run in a sensitivity investigation for the choice of the  $C_{\Delta}$  parameter required for the SGS model. This parameter controls the transport phenomena at sub-grid scales by controlling the sub-grid mixing length.

Fig. 6 shows the results of the analysis. All cases were run on grid level III. The results show that mean quantities are not affected significantly by varying  $C_{\Delta}$ ; furthermore, varying this parameter has different effects on different turbulence statistics. For example, while the effect on turbulence variances is minimal, the effect on turbulent fluxes are greater. The choices of  $C_{\Delta}$  provide reasonable simulation results in good agreement with the wind tunnel experiments.

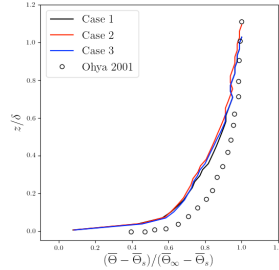
### F. Use of Wall Functions

Finally, the VLES model has been run in a sensitivity investigation when using wall functions. Here the first layer of the grid adjacent to the wall is gradually coarsened, which would correspond to increasing values of  $z^+$  in the simulation, while the quality of the solution is monitored. Fig. 7 shows the results of the analysis. All cases were run on grid level III. For these simulations, it was found that increasing the value of  $z^+$  does not degrade the quality of the mean solution obtained. However, with increasing values of  $z^+$ , turbulence statistics reduce and fluctuations are damped. It appears the  $z^+$  values up to 120 still provide reasonable agreement with the wind tunnel experiments.

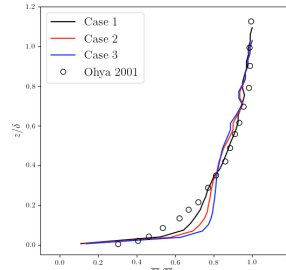
For use of wall functions, new choices of the synthetic eddy parameters must have been made for the simulations to perform adequately. Here, while we still used  $a_{\sigma}=3$ , we found that  $a_{\tau}=0.05$  would result in the best agreement. In other words, larger eddy lifetime must have been assumed for reasonable agreement with wind tunnel experiments. This can be explained by the fact that when wall functions are used, turbulence generation near the walls is modelled as opposed to resolved, in which case eddy formation at some distance away from the wall occurs with a larger time constant. This implies that TKE ( $k$ ) transfer from the wall to the outer layer starts with larger time constants, and therefore, it necessitates more model timestep iterations before new eddies are sampled at the Inlet [6].



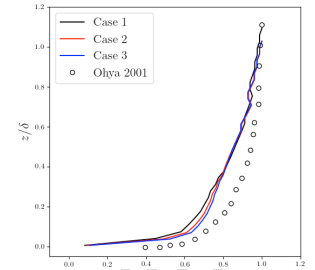
(a) Mean Velocity



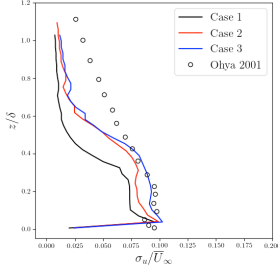
(b) Mean Temperature



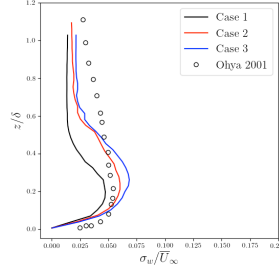
(a) Mean Velocity



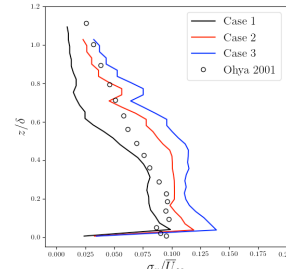
(b) Mean Temperature



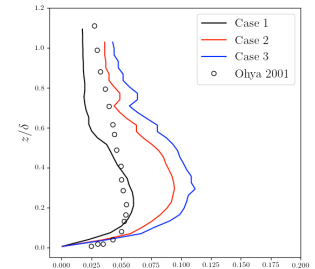
(c) Horizontal Velocity STD



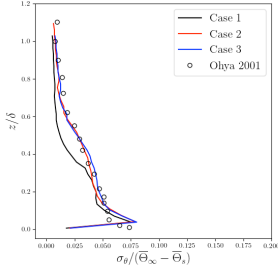
(d) Vertical Velocity STD



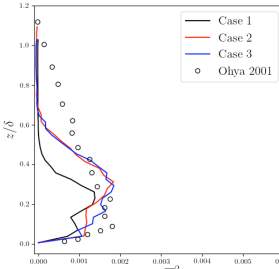
(c) Horizontal Velocity STD



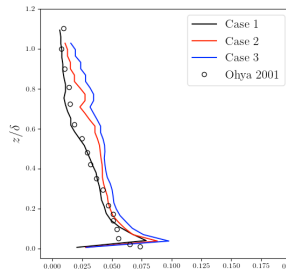
(d) Vertical Velocity STD



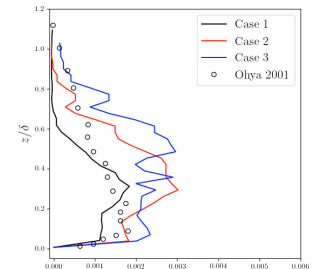
(e) Temperature STD



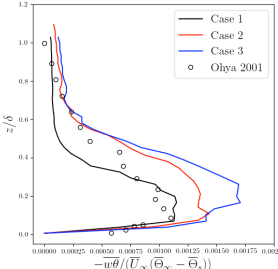
(f) Vertical Momentum Flux



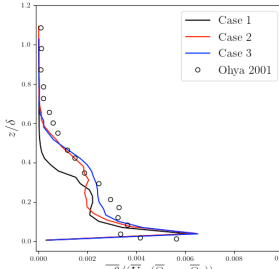
(e) Temperature STD



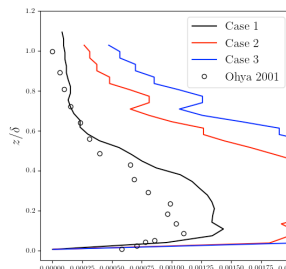
(f) Vertical Momentum Flux



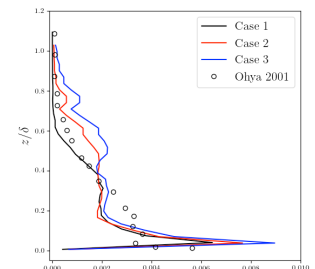
(f) Vertical Kinematic Heat Flux



(g) Horizontal Kinematic Heat Flux



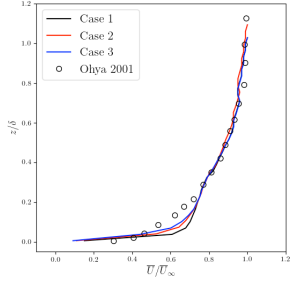
(f) Vertical Kinematic Heat Flux



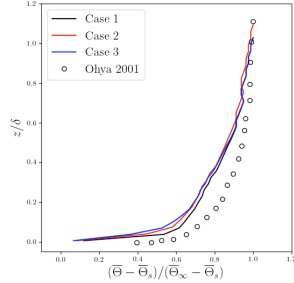
(g) Horizontal Kinematic Heat Flux

Figure 4. Sensitivity of the VLES model to different values of  $a_\sigma$ : Case 1 ( $a_\sigma=1$ ), Case 2 ( $a_\sigma=3$ ), and Case 3 ( $a_\sigma=5$ ).

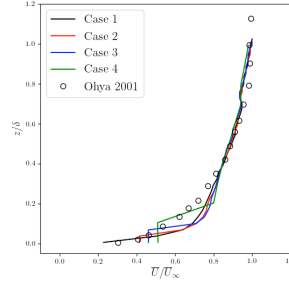
Figure 5. Sensitivity of the VLES model to different values of  $a_\tau$ : Case 1 ( $a_\tau=0.01$ ), Case 2 ( $a_\tau=0.05$ ), and Case 3 ( $a_\tau=0.1$ ).



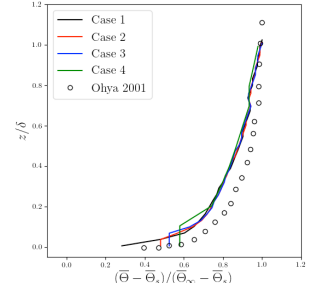
(a) Mean Velocity



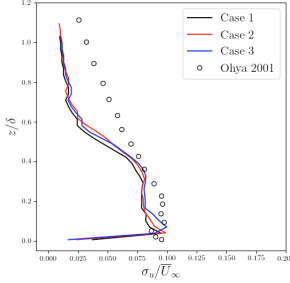
(b) Mean Temperature



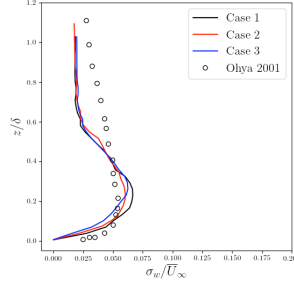
(a) Mean Velocity



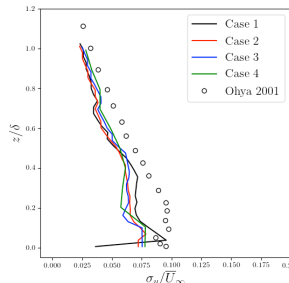
(b) Mean Temperature



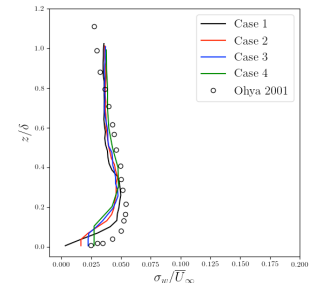
(c) Horizontal Velocity STD



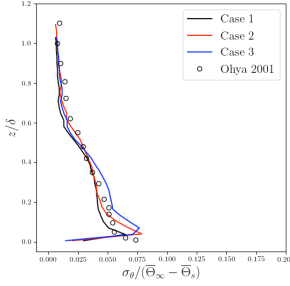
(d) Vertical Velocity STD



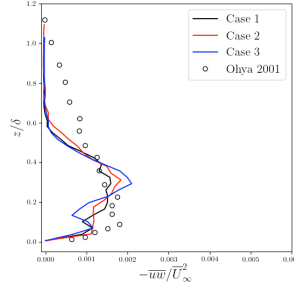
(c) Horizontal Velocity STD



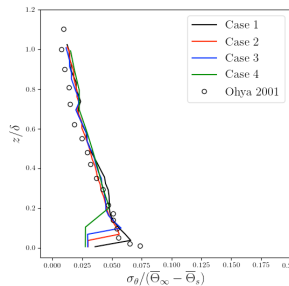
(d) Vertical Velocity STD



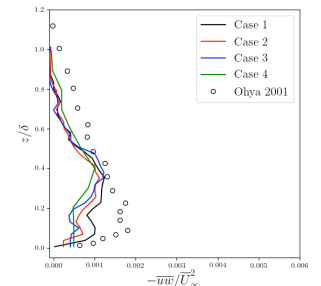
(e) Temperature STD



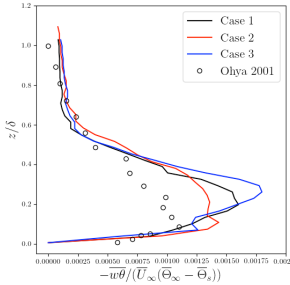
(f) Vertical Momentum Flux



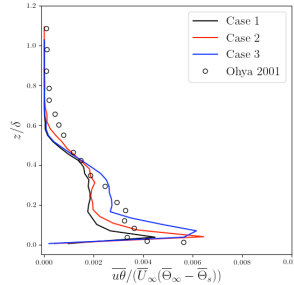
(e) Temperature STD



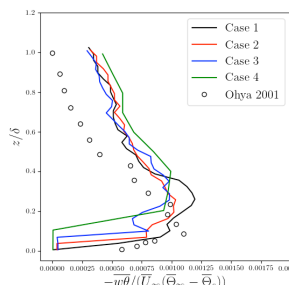
(f) Vertical Momentum Flux



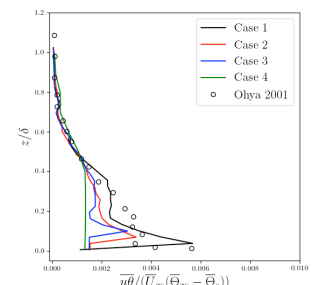
(f) Vertical Kinematic Heat Flux



(g) Horizontal Kinematic Heat Flux



(f) Vertical Kinematic Heat Flux



(g) Horizontal Kinematic Heat Flux

Figure 6. Sensitivity of the VLES model to different values of  $C_D$ : Case 1 ( $C_D=0.5$ ), Case 2 ( $C_D=1.0$ ), and Case 3 ( $C_D=1.5$ ).

Figure 7. Sensitivity of the VLES model to the first layer grid height when using wall functions: Case 1 ( $z^+ \sim 50$ ), Case 2 ( $z^+ \sim 80$ ), Case 3 ( $z^+ \sim 120$ ), and Case 4 ( $z^+ \sim 150$ ).

#### IV. CONCLUSIONS AND FUTURE WORK

A Very Large-Eddy Simulation (VLES) model was developed to simulate thermally-stratified atmospheric boundary layers. The model performance was validated against experimental thermal wind tunnel observations. The effect of grid resolution was analyzed. The model performance as a function of inlet parameters was studied in a sensitivity investigation. Various thermal stability strengths were analyzed. In addition, the model performance was investigated with the use of momentum and thermal wall functions.

The model exhibited a short adaptation distance smaller than five boundary-layer heights. It produced most of the mean and turbulence statistics profiles reasonably well. While turbulence statistics showed sensitivity to the choice of model parameters, the mean profiles were not so sensitive to such parameters. The choice of model parameters allowed an optimization to reach close agreement between the model and wind tunnel experiments. While the choice of wall functions implied reduced computational cost, the implementation of wall functions resulted in suppression of turbulence. Such suppression can further be circumvented by optimization of model parameters.

The VLES model shall be further tested at full scale to simulate thermally-stable atmospheric boundary layers. The model should also be tested on complex topography with differential surface temperature to ensure adequate performance in realistic applications.

#### ACKNOWLEDGEMENTS

In-kind technical support for this work was provided by Rowan Williams Davies and Irwin Inc. (RWDI). This work was supported by the Discovery Grant program (401231) from the Natural Sciences and Engineering Research Council (NSERC) of Canada; Government of Ontario through the Ontario Centres of Excellence (OCE) under the Alberta-Ontario Innovation Program (AOIP) (053450); and Emission Reduction Alberta (ERA) (053498). OCE is a member of the Ontario Network of Entrepreneurs (ONE). The computational platform was installed with the assistance of the IT team: Joel Best, Jeff Madge, and Matthew Kent.

#### REFERENCES

[1] H. Aboshosha, G. Bitsuamlak, and A. El Damatty, "LES of ABL flow in the built environment using roughness modeled by fractal surfaces," *Sustain. Cities Soc.*, vol. 19, pp. 40–60, 2015.

[2] H. Aboshosha, A. Elshaer, G. T. Bitsuamlak, and A. El Damatty, "Consistent inflow turbulence generator for LES evaluation of wind-induced responses for tall buildings," *J. Wind Eng. Ind. Aerod.*, vol. 142, pp. 198–216, 2015.

[3] A. A. Aliabadi, E. S. Krayenhoff, N. Nazarian, L. W. Chew, P. R. Armstrong, A. Afshari, and L. K. Norford, "Effects of roof-edge roughness on air temperature and pollutant concentration in urban canyons," *Boundary-Layer Meteorol.*, vol. 164, pp. 249–279, 2017.

[4] A. A. Aliabadi, *Theory and Applications of Turbulence: a Fundamental Approach for Scientists and Engineers*. Amir A. Aliabadi Publications, Guelph, 2018, pp. 168.

[5] A. A. Aliabadi, M. Moradi, D. Clement, W. D. Lubitz, and B. Gharabaghi, "Flow and temperature dynamics in an urban canyon under a comprehensive set of wind directions, wind speeds, and thermal stability conditions," *Environ. Fluid Mech.*, 2018 <https://doi.org/10.1007/s10652-018-9606-8>.

[6] A. A. Aliabadi, N. Veriotes, and G. Pedro, "A Very Large-Eddy Simulation (VLES) model for the investigation of the neutral atmospheric boundary layer," *J. Wind Eng. Ind. Aerod.*, vol. 183, pp. 152–171, 2018.

[7] S. Benhamadouche, N. Jarrin, Y. Addad, and D. Laurence, "Synthetic turbulent inflow conditions based on a vortex method for large-eddy simulation," *Prog. Comput. Fluid Dynam. Int. J.*, vol. 6, pp. 50–57, 2006.

[8] H. G. Castro, R. R. Paz, J. L. Mroginski, and M. A. Storti, "Evaluation of the proper coherence representation in random flow generation based methods," *J. Wind Eng. Ind. Aerod.*, vol. 168, pp. 211–227, 2017.

[9] C. L. V. Jayatilleke, "The influence of Prandtl number and surface roughness on the resistance of the laminar sub-layer to momentum and heat transfer," pp. 271, 1966.

[10] T. S. Lund, X. Wu, and K. D. Squires, "Generation of turbulent inflow data for spatially developing boundary layer simulations," *J. Comput. Phys.*, vol. 140, pp. 233–258, 1998.

[11] F. Mathey, D. Cokljat, J. P. Bertoglio, and E. Sergent, "Assessment of the vortex method for large eddy simulation inlet conditions," *Prog. Comput. Fluid Dynam. Int. J.*, vol. 6, pp. 58–67, 2006.

[12] Y. Ohya, "Wind-tunnel study of atmospheric stable boundary layers over a rough surface," *Boundary-Layer Meteorol.*, vol. 98, pp. 57–82, 2001.

[13] M. R. Raupach, R. A. Antonia, and S. Rajagopalan, "Rough-wall turbulent boundary layers," *Appl. Mech. Rev.*, vol. 44, pp. 1–25, 1991.

[14] M. Ricci, L. Patruno, and S. de Miranda, "Wind loads and structural response: benchmarking LES on a low-rise building," *Eng. Struct.*, vol. 144, pp. 26–42, 2017.

[15] M. E. Sergent, *Vers une methodologie de couplage entre la simulation des grandes echelles et les modeles statistique*, pp. 198, 2002.

[16] G. R. Tabor, and M. H. Baba-Ahmadi, "Inlet conditions for large eddy simulation: a review," *Comput. Fluids* vol. 39, pp. 553–567, 2010.

[17] T. G. Thomas, and J. J. R. Williams, "Generating a wind environment for large eddy simulation of bluff body flows," *J. Wind Eng. Ind. Aerod.*, vol. 82, pp. 189–208, 1999.

[18] B. Xie, "Improved Vortex Method for LES Inflow Generation and Applications to Channel and Flat-plate Flows," pp. 146, 2016.